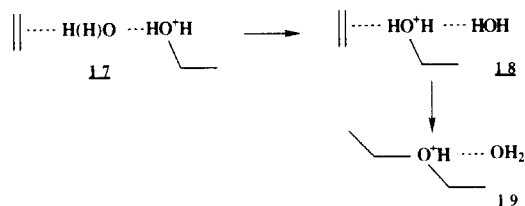


Figure 6. Estimated potential energy profile for the system $C_2H_5OH_2^+ + C_2H_5OH$.

Scheme III



+ 5 → 17. Transition-state energies have been obtained by using the homologous results presented in Tables III and IV.

As in the case of $(C_2H_5OH, H_2O)H^+$ adducts, the lack of observation of the dehydration products $C_2H_5OH_2^+ \rightarrow OH_2 + C_2H_4$,

despite a favorable thermochemistry ($\Delta H^\circ = 212$ kJ/mol, experimental value), is probably due to the high energy barrier associated with $14 \rightarrow 17$. Accordingly, considering the estimations presented in Figure 6, the transition state $14/17$ should lie in enthalpy near 290 kJ/mol, i.e., only slightly above the products $C_2H_5OH_2^+ + C_2H_5OH$.

In the same vein, the rearrangement $14 \rightarrow 17 \rightarrow 18 \rightarrow 19$ (Scheme III), which may also explain the formation of protonated diethyl ether by water loss, is not competitive with $15 \rightarrow 16$, as attested by the labeling results. This confirms the expectation of a large energy barrier for the process $14 \rightarrow 17$. Note that, similarly, $18 \rightarrow 19$ should also require a significant amount of energy.

In conclusion, the present study demonstrates that ion-neutral complexes are indeed stable species and may be involved during 1,2 elimination reactions from protonated alcohols. The structure of such complexes is a proton-bound association whose complexation energy, as estimated by high-level molecular orbital calculations, is ca. 70 kJ/mol.

The second important piece of information derived from calculation and experiment is that isomerization of the protonated form into its corresponding proton-bound complex, in the sense of Scheme 1, is associated with a high activation energy (greater than 120 kJ/mol). The transition-state energy levels seriously overlap those of the various dissociation products, a phenomenon therefore explaining the subtle balance between hydrogen exchanges and product branching ratios.

Photodissociation of a Bicyclic Azoalkane: Time-Resolved Coherent Anti-Stokes Raman Spectroscopy Studies of Vapor-Phase 2,3-Diazabicyclo[2.2.1]hept-2-ene

J. Stephen Adams,[†] R. Bruce Weisman,* and Paul S. Engel

Contribution from the Department of Chemistry and Rice Quantum Institute, Rice University, Houston, Texas 77251. Received May 29, 1990. Revised Manuscript Received August 3, 1990

Abstract: The photodissociative mechanism of vapor-phase 2,3-diazabicyclo[2.2.1]hept-2-ene (DBH) has been studied with nanosecond-regime transient spectroscopic methods. Following excitation of the vibrationless S_1 level at 338.5 nm, data from time-resolved CARS (a vibrational spectroscopy) show the appearance rate for formation of N_2 to be 4×10^7 s⁻¹. This value is significantly slower than the 5×10^8 s⁻¹ principal component observed in S_1 fluorescence decay, establishing that the dissociating state is not S_1 . CARS measurements on the nascent N_2 photofragments reveal a vibrational distribution (84% $v = 0$, 12% $v = 1$) very similar to that observed earlier for the nitrogen formed in the stepwise photodissociation of azomethane. This result and the low level of nascent rotational excitation suggest that dissociation into N_2 plus 1,3-cyclopentenediyl biradical occurs from an excited state of the diazenyl biradical that has a linear CNN bond angle. Transient CARS probing has also revealed the subsequent appearance of bicyclo[2.1.0]pentane formed by ring closure of the 1,3-cyclopentenediyl biradicals. Formation kinetics of this ring closure product shows a single first-order component with a rate coefficient of approximately 5.1×10^6 s⁻¹. This observation implies that S_1 excitation of vapor-phase DBH produces 1,3-cyclopentenediyl biradicals only in their ground triplet state. Mechanistic differences between the gas-phase photochemistries of DBH and acyclic azoalkanes are attributed to a low-lying excited state of the diazenyl biradical that becomes accessible in DBH through the release of ring strain energy.

Introduction

Although the thermal and photochemical dissociation of azoalkanes into nitrogen plus alkyl radicals ($RN=NR' \rightarrow R + N_2 + R'$) has been observed for decades,¹ the mechanisms of these processes generally remain unclear and somewhat controversial.² Research in this area centers on determining whether the two C-N

bonds break in a single step or in two, identifying and characterizing any reaction intermediates and, in the case of photolysis, understanding the roles played by various electronic states.

Among azoalkanes, the cyclic compounds (those having covalent bonds linking R and R') command special attention for two reasons. First, the notable differences between their dissociative

[†] Present address: Naval Research Laboratory, Code 6110, Washington, DC 20375.

(1) Ramsperger, H. C. *J. Am. Chem. Soc.* **1927**, *49*, 912.

(2) Engel, P. S. *Chem. Rev.* **1980**, *80*, 99.

behavior and that of the acyclics may provide clues for uncovering key structural and energetic factors governing dissociation of all azoalkanes. Second, the loss of N_2 from cyclic azoalkanes provides an efficient and clean method for producing biradicals of great current interest.³

The present investigation concerns the gas-phase photochemistry of 2,3-diazabicyclo[2.2.1]hept-2-ene (DBH), a bicyclic azoalkane first synthesized in 1957.⁴ In 1968, Solomon, Thomas, and Steel reported a broad range of photophysical and photochemical measurements on DBH, including absorption, emission, and fluorescence excitation spectra, and the pressure-dependent yields for fluorescence and photodissociation.⁵ These results showed that, unlike its acyclic counterparts, vapor-phase DBH exhibits a structured rather than a diffuse $S_1 \leftarrow S_0$ absorption spectrum and fluoresces measurably from its n, π^* S_1 state (with a quantum yield of 1.4×10^{-2}). Like the acyclics at low pressures, vapor-phase DBH photodissociates from its S_1 state with a quantum yield of nearly 1. However, DBH again differs from the acyclics by retaining its high photodissociative yield in solution, even though its fluorescence is strongly quenched. Solomon et al. concluded that the photochemistry of DBH occurs through pressure-induced dissociation from the excited singlet state. The triplet state is also dissociative both in the gas phase and in solution, but the differing product distributions obtained in solution by direct and triplet-sensitized photolysis of substituted DBHs speak against intersystem crossing prior to loss of nitrogen.⁶⁻¹⁰

In a 1979 study that exploited the potential of bicyclic azoalkanes to form biradicals, Buchwalter and Closs photolyzed matrix-isolated DBH and observed ESR spectra of the resulting triplet 1,3-cyclopentadienyl (CPD).¹¹ Temperature-dependent studies of the ESR signals from this biradical provided an estimate of its activation barrier for decay into bicyclopentane. More recently, Adam and co-workers have used stereochemical product analysis to investigate the thermal and photochemical dissociation mechanisms of deuterated and substituted DBHs in solution.⁹ They have deduced a mechanistic scheme based on qualitative features of electronic states of DBH and its product biradicals that accounts for their experimental findings. The scheme proposed by these workers shows different dissociation pathways for thermally excited, triplet-sensitized, near-UV-excited, and vacuum-UV-excited DBH molecules.⁹

A different approach for distinguishing synchronous from stepwise molecular elimination in DBH and certain other compounds was proposed in 1969 by Bauer.¹² He suggested analyzing the vibrational energy content of the nascent N_2 , which would be formed with high vibrational excitation only if both C-N bonds break in a single step, thereby causing an abrupt change in the equilibrium N-N separation. The N_2 would not transfer this "Franck-Condon" vibrational excitation to the hydrocarbon fragment because the N-N axis would be orthogonal to the reaction coordinate. Although Bauer did not comment on rotational distributions, it is also clear that synchronous dissociation through a symmetrical transition state would exert equal forces on the two

nitrogen centers and avoid rotational excitation of the nascent N_2 .

In the period since Bauer's suggestion, the use of fragment energy distributions to infer dissociation dynamics has become more experimentally feasible.¹³ Studies in our laboratory using time-resolved CARS, a vibrational probe spectroscopy, have directly revealed stepwise photodissociation kinetics in an unsymmetrical acyclic azoalkane¹⁴ and, recently, in azomethane.¹⁵ Moreover, this method has provided the nascent vibrational¹⁶ and rotational^{17,18} distributions of N_2 from azomethane. Because it is now clear that these N_2 distributions result from dissociation of methyldiazanyl radicals as the second C-N bond cleaves, it is possible to use nascent N_2 distributions measured for other azoalkanes to deduce their photodissociation mechanisms with reasonable confidence.

We describe here the results of time-resolved spectroscopic experiments on vapor-phase DBH that reveal internal state distributions of the nitrogen as well as formation kinetics of the stable photoproducts. When combined with theoretical considerations, these results lead to novel insights into the pathways of DBH photodissociation. In addition, we report the lifetime against ring closure of the triplet 1,3-cyclopentadienyl biradical. Finally, an explanation is proposed for photochemical differences between DBH and the acyclic azoalkanes.

Experimental Method

The apparatus and methods used in our laboratory for transient coherent anti-Stokes Raman spectroscopy (CARS)¹⁹ have been described in some detail previously.^{15,20} In the present studies, static gas-phase samples containing 0.7-1.0 Torr DBH at 295 ± 2 K were excited at the 338.5-nm origin band of the $S_1 \leftarrow S_0$ n, π^* transition. The 338.5-nm excitation pulses were generated by frequency doubling the output of a tunable dye laser that used the 532-nm second harmonic of a Q-switched Nd:YAG laser to pump DCM dye in DMSO solution.

Following each excitation pulse, a second Q-switched Nd:YAG/dye laser system was fired after an electronically controlled nanosecond-scale time delay. This second laser system produced two synchronized CARS probing pulses whose frequency difference defined the Raman frequency that was monitored. We measured induced CARS signals from optically excited samples either as a function of delay after excitation (with fixed probe frequency) or as a function of Raman frequency (with fixed probe delay). Typically, ca. 20% of the sample molecules within the probed volume absorbed light from the excitation pulse. During the 100-ms laser repetition interval, diffusion between the small probed volume and the full sample cell volume tended to restore the probed volume to its initial composition. The optical geometry was the "folded BOXCARS" arrangement used in recent studies from this laboratory.^{20,21} Because none of the photoproduct species monitored in this work have electronic absorptions near the CARS probing wavelengths, there was no electronic resonance enhancement of their CARS signal strengths. The instrumental time response of the apparatus was approximately 8 ns FWHM, and its spectral resolution was ca. 1 cm^{-1} . Capacitance manometers were used to measure the pressures of sample and added buffer gases. Our DBH samples were synthesized from the Diels-Alder adduct of cyclopentadiene and diethyl azodicarboxylate according to the literature procedure.²²

We performed kinetic analysis of time-resolved CARS data using a Marquardt optimization program that adjusted selected rate coefficients within a specified kinetic model to obtain the best least-squares agreement between simulated and measured data. During this analysis, the

(3) (a) Borden, W. T., Ed. *Diradicals*; Wiley: New York, 1982. (b) Michl, J., Ed. *Tetrahedron* **1982**, *38*(4), 733 (Symp. Print). (c) Adam, W.; Plaisch, H.; Wirz, J. *J. Am. Chem. Soc.* **1989**, *111*, 6896. (d) Snyder, G. J.; Dougherty, D. A. *J. Am. Chem. Soc.* **1989**, *111*, 3927. (e) Roth, W. R.; Bauer, F.; Braun, K.; Offerhaus, R. *Angew. Chem., Int. Ed. Engl.* **1989**, *28*, 1056. (f) Stone, K. J.; Greenberg, M. M.; Blackstock, S. C.; Berson, J. A. *J. Am. Chem. Soc.* **1989**, *111*, 3659. (g) Ham, S. W.; Chang, W.; Dowd, P. *J. Am. Chem. Soc.* **1989**, *111*, 4130.

(4) Criegee, R.; Rimmelin, A. *Chem. Ber.* **1957**, *90*, 414.

(5) Solomon, B. S.; Thomas, T. F.; Steel, C. *J. Am. Chem. Soc.* **1968**, *90*, 2249.

(6) Allred, E. L.; Smith, R. L. *J. Am. Chem. Soc.* **1969**, *91*, 6766.

(7) Roth, W. R.; Enderer, K. *Justus Liebig's Ann. Chem.* **1970**, *733*, 44.

(8) Turro, N. J.; Renner, C. A.; Waddell, W. H.; Katz, T. J. *J. Am. Chem. Soc.* **1976**, *98*, 4320.

(9) Adam, W.; Oppenlander, T.; Zang, G. *J. Org. Chem.* **1985**, *50*, 3303.

(10) Culotta, A. M.; Engel, P. S. *Abstracts of Papers*, 197th National Meeting of the American Chemical Society, Dallas, TX; American Chemical Society: Washington, DC, 1989; ORGN 198. Engel, P. S.; Culotta, A. M. *J. Am. Chem. Soc.*, in press.

(11) Buchwalter, S. L.; Closs, G. L. *J. Am. Chem. Soc.* **1979**, *101*, 4688.

(12) Bauer, S. H. *J. Am. Chem. Soc.* **1969**, *91*, 3688.

(13) (a) Debarre, D.; Lefebvre, M.; Pealat, M.; Taran, J.-P. E.; Bamford, D. J.; Moore, C. B. *J. Chem. Phys.* **1985**, *83*, 4476. (b) Moore, C. B.; Bamford, D. *Laser Chem.* **1986**, *6*, 93. (c) Schinke, R. *J. Chem. Phys.* **1986**, *84*, 1487.

(14) Adams, J. S.; Burton, K. A.; Andrews, B. K.; Weisman, R. B.; Engel, P. S. *J. Am. Chem. Soc.* **1986**, *108*, 7935.

(15) Burton, K. A.; Weisman, R. B. *J. Am. Chem. Soc.* **1990**, *112*, 1804.

(16) Holt, P. L.; McCurdy, K. E.; Adams, J. S.; Burton, K. A.; Weisman, R. B.; Engel, P. S. *J. Am. Chem. Soc.* **1985**, *107*, 2180.

(17) Burton, K. A. Ph.D. Thesis, Rice University, September 1989.

(18) Burton, K. A.; Andrews, B. K.; Weisman, R. B. To be published.

(19) Tolles, W. M.; Nibler, J. W.; McDonald, J. R.; Harvey, A. B. *Appl. Spectrosc.* **1977**, *31*, 253.

(20) Stout, J. E.; Andrews, B. K.; Bevilacqua, T. J.; Weisman, R. B. *Chem. Phys. Lett.* **1988**, *151*, 156.

(21) Shirley, J. A.; Hall, R. J.; Eckbreth, A. C. *Opt. Lett.* **1980**, *5*, 380.

(22) Gassman, P. G.; Mansfield, K. T. *Organic Syntheses*; Wiley: New York, 1973; Collect. Vol. V, p 96.

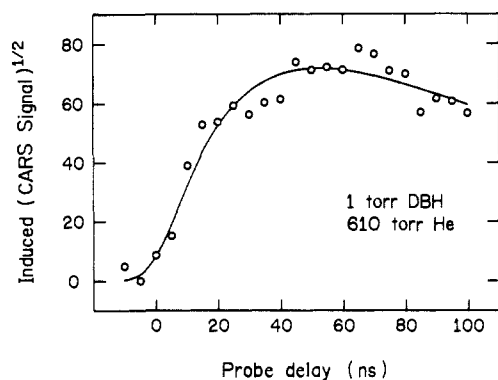


Figure 1. N_2 population kinetics measured for samples containing 1 Torr DBH plus 610 Torr helium. The smooth curve is a kinetic simulation computed as described in the text. The deduced unimolecular appearance rate is $4 \times 10^7 \text{ s}^{-1}$.

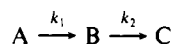
kinetic rate equations were numerically integrated for each set of rate coefficients and the resulting concentration history was convoluted with a Gaussian representing the instrumental time response function.

Fluorescence lifetime data were obtained with a time-correlated single-photon counting apparatus at the Center for Fast Kinetics Research in Austin, TX. The 338.5-nm excitation source was the second harmonic of a Spectra Physics dye laser run with pyridine-I dye and synchronously pumped by 532-nm pulses from a mode-locked CW Nd:YAG laser. The dye laser produced 12-ps pulses at its cavity-dumping repetition rate of 800 kHz. A long-pass interference filter in front of the detector blocked scattered excitation light while passing fluorescence at wavelengths greater than approximately 370 nm. The sample cell contained 0.2 Torr of a DBH sample found to be more than 99.6% pure by differential scanning calorimetry. We analyzed the fluorescence kinetics using data beyond the decay of the instrumental response function, whose width was approximately 1 ns FWHM.

Results

To measure the kinetics of N_2 formation from photoexcited DBH, we monitored induced CARS signals from nitrogen's well-known $0 \leftrightarrow 1$ vibrational band, whose origin frequency is 2329.8 cm^{-1} .²³ The data acquisition methods described for the azomethane CARS studies were also applied here to compensate for signal contributions from nitrogen formed in earlier laser shots and for the nonlinear spectral distortions caused by buffer gases.¹⁵ Even with these methods, we obtain population kinetics only for a narrow range of quantum states whose spectral transitions fall within the probed frequency range. To ensure that the measured kinetics reflect chemical formation of nitrogen rather than collisional energy relaxation, it is therefore necessary to use sample conditions that give steady rotational and vibrational distributions on the time scale of our measurements. Such steady distributions will occur for very rapid thermalization and also for very slow relaxation.

Figure 1 shows the nitrogen population growth measured from 1 Torr DBH in the presence of 610 Torr helium buffer gas. This pressure of helium should cause rotational relaxation in slightly less than 1 ns and vibrational relaxation in several milliseconds.²⁴ Therefore, on the time scale of our measurement the nitrogen internal energy distributions remain virtually static: the rotational populations are kept thermalized and the vibrational populations are frozen in their nascent distribution. The solid curve drawn through the data points shows a best fit computed by using the simple kinetic model:



Here B is the nitrogen photoproduct, A represents its precursor, and C is an "invisible" species. The step from B to C lets us model the artificial decrease in signal that occurs when preexisting nitrogen molecules suffer collisions with translationally excited

Table I. Nascent Vibrational Distribution of the N_2 Photoproduct

vibrational quantum no.	measured population ^a	computed population ^b
0	0.84	0.86
1	0.12	0.13
2	0.04	0.01

^a Estimated experimental uncertainties, ± 0.04 . ^b Using the Franck-Condon projection method described in the text and assuming a bond length contraction of 2.8 pm.

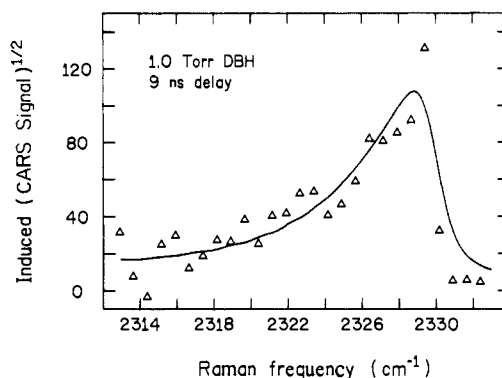


Figure 2. Induced CARS spectrum of the $\nu = 0 \leftrightarrow 1$ band of nitrogen photoproduct measured at a probe delay of 9 ns in samples containing 1 Torr DBH with no buffer gas. The solid curve is a computed CARS spectrum of N_2 at a rotational temperature of 550 K.

photofragments.¹⁵ We find k_1 , the first-order rate coefficient for production of N_2 , to be $4.0 (\pm 1) \times 10^7 \text{ s}^{-1}$, corresponding to a precursor lifetime of 25 ns.

To determine the nascent vibrational distribution of the N_2 photoproduct, we performed spectral scans at a probe delay of 50 ns in samples containing 1 Torr DBH plus 610 Torr helium. As discussed above, these conditions ensure the collapse of vibration-rotation band contours to their thermal widths but preserve the initial distribution of population among the various vibrational states. Vibrational anharmonicity separates nitrogen's $0 \leftrightarrow 1$, $1 \leftrightarrow 2$, and $2 \leftrightarrow 3$ band origins by intervals of ca. 28 cm^{-1} ,²³ so these bands are readily distinguished and quantified in the transient CARS spectrum. All three bands showed dispersive line shape components whose signs imply the absence of population inversions. No evidence was found for transitions involving higher vibrational states. In deducing the vibrational population distribution from CARS signal strengths, we assumed that the Raman cross sections are proportional to the upper state vibrational quantum number, as is the case for harmonic oscillators.²⁵ The results of this analysis are shown in Table I.

In contrast to these vibrational measurements, the nascent rotational population distribution of N_2 photoproduct must be measured under precollisional conditions in order to avoid errors caused by efficient rotational relaxation. Experimentally, precollisional conditions require low sample pressures, no buffer gas, and probe delays as small as possible. Signal strength limitations prevented us from making these measurements with DBH pressures below 1 Torr or at delays of less than 9 ns (at which time only half of the N_2 has appeared). Because nitrogen molecules moving with thermal velocities in 1 Torr DBH have a mean time between hard-sphere collisions of approximately 95 ns, a probe delay of 9 ns would seem safely precollisional. However, our low-pressure data on nitrogen appearance kinetics show evidence of more rapid collisional processes that we attribute to high translational energy in the N_2 photofragment. This means that the first collision interval is considerably shorter than 95 ns. We estimate that our observations of nitrogen spectra at 9-ns probe delay are mainly, although not entirely, precollisional.

The nitrogen rotational excitation was assessed from the contour of the $\nu = 0 \leftrightarrow 1$ band measured with a spectral resolution of 1

(23) Rosen, B. *Spectroscopic Data Relative to Diatomic Molecules*; Pergamon: Oxford, 1970.

(24) Lambert, J. D. *Vibrational and Rotational Relaxation in Gases*; Clarendon: Oxford, 1977; p 29.

(25) Graybeal, J. D. *Molecular Spectroscopy*; McGraw-Hill: New York, 1988.

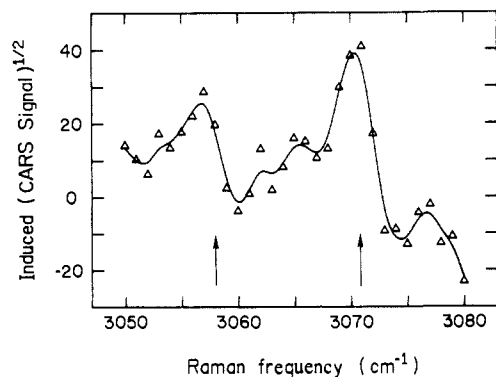


Figure 3. Induced CARS spectrum of a portion of the C-H stretching region measured 500 ns after excitation in samples containing 0.7 Torr DBH plus 600 Torr helium buffer. The points show measured data and the solid line is a spline fit intended as a visual guide. For comparison, the band centers of authentic BCP transitions are marked with arrows.

cm⁻¹. Figure 2 shows the experimental data along with a simulated spectral contour computed for nitrogen at a rotational temperature of 550 K. Although this temperature was found to give the most satisfactory match to the observed contour data, we believe for the following reasons that 550 K represents an upper limit to the actual nascent rotational excitation. At later probe delays we find band contours corresponding to *higher* rotational temperatures. Two effects may explain this observation. First, on collision with a DBH molecule, a rapidly moving photoproduct N₂ can convert its translational energy into rotational excitation with the high efficiencies characteristic of R → T collisional relaxation. At delays somewhat greater than 9 ns, a larger fraction of the emerging molecules will have suffered a first collision and had the opportunity to gain rotational excitation. The second effect involves collisions between rapidly moving nitrogen molecules and thermalized nitrogen formed from earlier laser shots. If the thermalized molecules become rotationally excited by collisional T → R energy transfer, then the induced CARS spectrum will show depleted signals at low *J* values and excess signals at high *J* values. The result of these two related collisional effects is to distort the measured spectrum in the direction of increased rotational temperature. We conclude that the unperturbed N₂ molecules produced in DBH photolysis have less rotational excitation than that of a Boltzmann distribution at 550 K.

Fluorescence lifetime measurements were made following S₁ origin excitation of DBH at 0.2 Torr. The resulting data showed nonexponential decay that could be decomposed into the sum of two exponential components. The main decay component had a rate coefficient of 4.85 (±0.7) × 10⁸ s⁻¹, while the second component, whose amplitude was smaller by a factor of 28, showed a coefficient of 1.47 (±0.3) × 10⁸ s⁻¹. These values correspond to 1/*e* decay times of 2.1 and 6.8 ns for the major and minor components.

Photolysis of DBH is known to produce bicyclo[2.1.0]pentane (BCP) in addition to nitrogen. Ground-state CARS spectra of DBH samples exposed to prolonged irradiation in our sample cell showed several sharp permanent photoproduct bands whose frequencies agree well with those reported for the Raman spectrum of BCP.²⁶ This identification of the photoproduct as BCP was confirmed by scanning the ground-state CARS spectrum of an authentic sample of BCP. Induced CARS spectra measured 500 ns after excitation in samples containing 0.7 Torr DBH plus 600 Torr helium buffer gas showed positive-going transient signals peaking at 971, 2873, 2920, 2945, 3057, and 3070 cm⁻¹. Each of these frequencies matches a strong ground-state CARS transition of BCP and agrees within our calibration uncertainty with a reported vapor-phase Raman frequency. Figure 3 shows a portion of the transient spectrum measured in the C-H stretching region, with the positions of ground-state BCP bands marked for comparison.

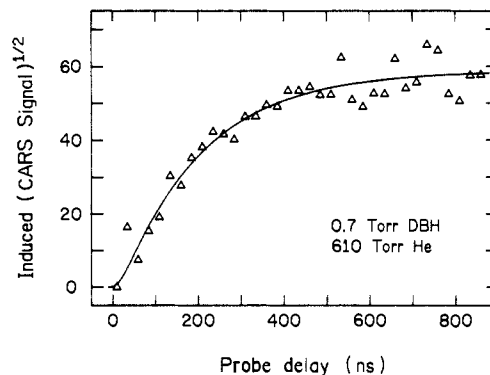
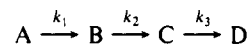


Figure 4. BCP population kinetics measured at 3070 cm⁻¹ in samples containing 0.7 Torr DBH plus 605 Torr helium. The smooth curve is a kinetic simulation computed as described in the text. The deduced unimolecular formation rate of BCP is 5.1 (±0.5) × 10⁶ s⁻¹.

In order to monitor the appearance of BCP following excitation of DBH, we collected kinetic CARS data at a probe frequency of 3070 cm⁻¹ in samples containing 0.7 Torr DBH plus 605 Torr helium added to induce rotational and vibrational relaxation. (Although ineffective at deactivating N₂ vibrations, helium should induce vibrational relaxation of BCP because of the far denser vibrational manifold; each BCP molecule suffers 11 hard-sphere collisions per nanosecond.) The 3070-cm⁻¹ data on BCP appearance, shown in Figure 4, were analyzed by using the following three-step kinetic model:



Here, the first step represents dissociation of excited DBH to form nitrogen plus the biradical precursor of BCP, the second step represents ring closure of the biradical to form BCP, and the third step (to an "undetectable" product) accounts for possible loss of BCP from the probed volume through heating effects. On the basis of analysis of N₂ appearance kinetics described earlier, we fixed *k*₁ at 4.0 × 10⁷ s⁻¹ and allowed *k*₂ and *k*₃ to be optimized. The optimal value of *k*₃ was found to be negligibly small and *k*₂ was found to be 5.1 (±0.5) × 10⁶ s⁻¹. This value corresponds to a lifetime of approximately 195 ns for the precursor of BCP.

Discussion

The fluorescence lifetime results show that vapor-phase DBH excited to the origin of its S₁ state has a collision-free lifetime of slightly more than 2 ns. This value is smaller than the one estimated by Solomon et al.⁵ based on the fluorescence quantum yield and an oscillator strength determined with the Strickler-Berg formula. Solomon et al. found collisional quenching of DBH fluorescence, with 50% of the emission quenched by 1210 Torr nitrogen. On the basis of the buffer pressures used in our experiments and the lower quenching efficiency expected for helium compared to nitrogen, we believe that all of the measurements reported here are dominated by the unquenched, "low-pressure" decay channel of S₁ DBH.

When the ca. 2-ns decay lifetime of the S₁ state is compared with the 25-ns appearance time of free N₂, it seems clear that low-pressure S₁ DBH does not decay directly into separated photodissociation products. Instead, the products of S₁ decay might be a triplet state of DBH or various states of the diazenyl biradical that would be formed by breaking one C-N bond. In Figure 5 we present the energies and some adiabatic correlations of species that may be involved in the S₁ photochemical mechanism of DBH. The energetic data were obtained from reported spectroscopic,⁵ calorimetric,²⁷⁻²⁹ and kinetics experiments^{11,30,31} plus unpublished ab initio model computations from our laboratory.³²

(27) Engel, P. S.; Melaugh, R. A.; Mansson, M.; Timberlake, J. W.; Garner, A. W.; Rossini, F. D. *J. Chem. Thermodyn.* **1976**, *8*, 607.

(28) Chang, S.; McNally, D.; Tehrani, S. S.; Hickey, M. J.; Bold, R. H. *J. Am. Chem. Soc.* **1970**, *92*, 3109.

(29) Herman, M. S.; Goodman, J. L. *J. Am. Chem. Soc.* **1988**, *110*, 2681.

(30) Engel, P. S. *J. Am. Chem. Soc.* **1969**, *91*, 6903.

(31) Cohen, S. G.; Zand, R.; Steel, C. *J. Am. Chem. Soc.* **1961**, *83*, 2895.

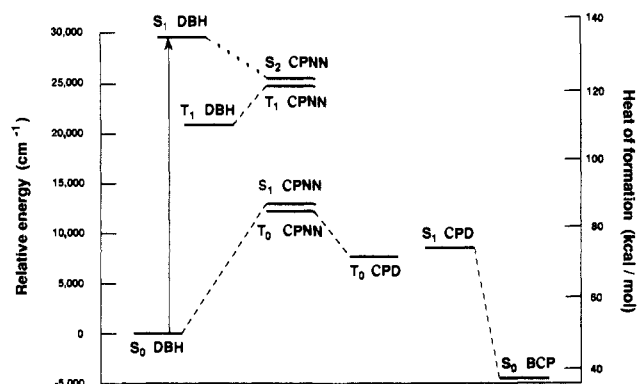


Figure 5. Vapor-phase energetics of states and species that may be involved in the S_1 photolysis of DBH. CPNN denotes the diazenyl biradical formed by breaking one C–N bond in DBH; CPD is the 1,3-cyclopentadienyl biradical; and BCP is bicyclopentane.

Dashed lines indicate adiabatic correlations between states, but we have not attempted to illustrate the energy profiles along reaction coordinates between species.

Of the several pathways that can be imagined for forming BCP plus N_2 from the S_1 state of DBH, some may be excluded on the basis of our transient CARS data. The appearance kinetics observed for BCP implies that its precursor, which must be some state of the CPD biradical, has a lifetime near 195 ns. If this biradical were present as a singlet, it would almost surely decay by ring closure in a time far shorter than 195 ns. We therefore conclude that the lifetime is that of CPD's triplet ground state, whose closure to S_0 BCP is delayed by the need for a spin change as well as geometrical distortion. Our inferred 195-ns lifetime for T_0 CPD lies in the range of previously reported values determined indirectly in room-temperature solution: >100 ns from oxygen quenching studies,³³ 100 ns from oxygen trapping studies,³⁴ and 316 ± 80 ns from photoacoustic measurements.²⁹ Another comparison may be made using the Arrhenius parameters reported by Buchwalter and Closs in their ESR study of triplet CPD. From decay kinetics of biradical ESR signals measured over a limited range of low temperatures, these workers deduced an Arrhenius A factor of 10^8 s⁻¹ and an activation energy of 2.3 ± 0.2 kcal/mol,¹¹ which when applied at 295 K predict a T_0 CPD lifetime between 355 and 505 ns. Again, we consider this value to be in reasonable agreement with our result in view of the large temperature extrapolation and possible differences between condensed- and gas-phase behaviors.

Our data on the appearance kinetics of BCP show that this product is formed not through the singlet state of the CPD biradical, which would undergo very rapid ring closure, but instead through triplet CPD. The propensity for spin conservation in dissociation then implies that T_0 CPD is probably produced through loss of nitrogen from a triplet precursor. What are the candidates for this dissociating precursor to T_0 CPD? Figure 5 shows three: T_1 DBH, the lowest triplet state of "CPNN" (the diazenyl biradical formed by breaking one C–N bond of DBH), and the first excited triplet state of CPNN. Diazenyl-alkyl biradicals have been postulated previously in the photolysis of several cyclic azoalkanes.^{35–37}

It is possible to distinguish among these three possible dissociative pathways by using the nascent rotational and vibrational distributions observed for the N_2 photoproduct. We expect that the vibrational distribution will be controlled mainly by the difference in N–N separation between the dissociative transition state or critical geometry and the free nitrogen molecule. Vibrational population distributions for the photoproduct N_2 can be simulated

with a simple Franck–Condon projection model. In this model, harmonic oscillator wave functions for various vibrational levels of the free N_2 molecule are multiplied by a $v = 0$ harmonic oscillator wave function whose equilibrium separation and frequency represent the N_2 structure just before dissociation occurs. Integrals over the products of these wave functions are then squared to obtain Franck–Condon factors giving the probabilities of forming the N_2 photoproduct in various vibrational states. As shown in Table I, the observed vibrational distribution is very well fit by a model calculation in which the bond length at the transition state or critical geometry exceeds that of free N_2 by approximately 0.028 Å. Note that this value is only $\sim 19\%$ of the 0.148-Å total change in N–N bond length that occurs in going from ground-state DBH (1.246 Å)³⁸ to N_2 (1.098 Å).²³ From the near-mirror symmetry of DBH absorption and fluorescence spectra and the molecule's rigid structure, we infer that the lowest n,π^* states have essentially the same geometry as the DBH ground state. Single-step dissociation from T_1 DBH into N_2 plus T_0 CPD would therefore involve a very large change in N–N separation that would almost surely yield a hotter vibrational distribution than we observe. Stated differently, the measured N_2 vibrational distribution implies a critical structure so different from the intact DBH molecule that the T_1 state of DBH could not feasibly distort into that dissociative geometry. In addition, the nitrogen vibrational distribution from DBH is very similar to that found from azomethane photolysis,¹⁶ a process now known to proceed through a methyldiazenyl radical intermediate.¹⁵ It should also be noted that recent shock tube experiments on DBH thermolysis indicate a nascent N_2 vibrational distribution similar to our photolysis findings.³⁹ This suggests that thermolysis also proceeds through a diazenyl biradical intermediate, presumably the S_1 state of CPNN.

Having ruled out the lowest triplet state of DBH as the photodissociating species, and with it the possibility of synchronous two-bond cleavage, can we discriminate between the ground and first excited states of the CPNN biradical? An important clue is the "cool" (less than 550 K) rotational temperature of the nascent nitrogen. This temperature contrasts sharply with the 2000–2500 K values found in nitrogen formed from such acyclic azoalkanes as azomethane and 2-azopropane.¹⁷ We interpret the rotational excitation level as a measure of the torque exerted on the nitrogen molecule by repulsive forces acting as it leaves the transition-state region. If these forces are exerted equally on both nitrogen atoms, as in synchronous cleavage of both C–N bonds of DBH, there will be no net torque. If dissociation occurs from a diazenyl radical transition state with a strongly bent C–N–N bond angle, there will be considerable torque and rotational excitation. Finally, if dissociation occurs from a diazenyl radical with a linear C–N–N bond angle, there will be no torque and the departing N_2 will receive translational rather than rotational excitation.

To proceed further we must consider structures and energies of the CPNN diazenyl biradical. We will make the crucial but very plausible assumption that the diazenyl group of CPNN is largely unaffected by the second, rather distant radical center, so that its electronic states will resemble those of other alkyldiazenyl radicals. There is a firm theoretical expectation that the C–N–N bond angle of simple diazenyl radicals will be strongly bent in the ground state and linear in the lowest excited state, which corresponds to excitation of the radical electron from a σ to a π orbital.^{40,41} Ab initio CASSCF calculations⁴² in our laboratory have indeed found C–N–N angles of 120° and 180° for the ground and first excited states of methyldiazenyl.³² On the basis of the small coupling expected between the two radical centers in CPNN, we presume that the singlet and triplet states

(32) Andrews, B. K.; Weisman, R. B. To be published.

(33) Clark, W. D. K.; Steel, C. J. *Am. Chem. Soc.* **1971**, *93*, 6347.

(34) Adam, W.; Hossel, P.; Hummer, W.; Platsch, H.; Wilson, R. M. J. *Am. Chem. Soc.* **1987**, *109*, 7570.

(35) Reedich, D. E.; Sheridan, R. S. J. *Am. Chem. Soc.* **1988**, *110*, 3697.

(36) Adam, W.; Gillaspay, W. D.; Peters, E.-M.; Peters, K.; Rosenthal, R. J.; von Schnring, H. G. J. *Org. Chem.* **1985**, *50*, 580.

(37) Adam, W.; Dorr, M. J. *Am. Chem. Soc.* **1987**, *109*, 1240.

(38) Suenram, R. D. *J. Mol. Struct.* **1976**, *33*, 1.

(39) Simpson, C. J. S. M., Oxford University, personal communication, 1990.

(40) Bigot, B.; Sevin, A.; Devaquet, A. J. *Am. Chem. Soc.* **1978**, *100*, 2639.

(41) Baird, N. C.; Kathpal, H. B. *Can. J. Chem.* **1977**, *55*, 863.

(42) For a review, see: Roos, B. O. In *Ab Initio Methods in Quantum Chemistry*; Lawley, K. P., Ed.; Wiley: New York, 1987; Vol. II, p 399.

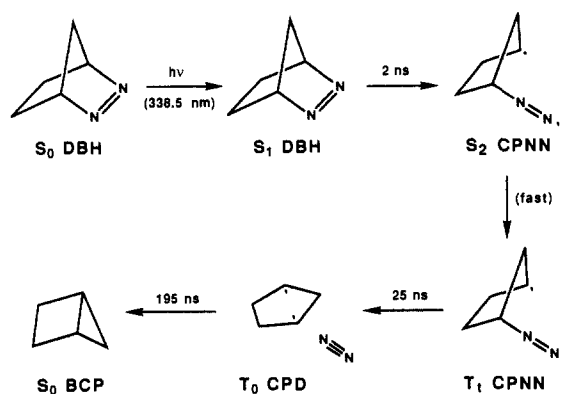


Figure 6. Schematic illustration of the proposed photolysis mechanism for vapor-phase DBH excited to the origin level of its S_1 state.

arising from the same diazenyl electronic configuration are nearly degenerate, with the triplet state lying slightly lower because of Hund's rule. CASSCF calculations find the energy separation between equilibrium geometries of the ground and first excited states of methyldiazenyl to be approximately $12\,700\text{ cm}^{-1}$ (36 kcal/mol).³² As shown in Figure 5, applying this methyldiazenyl energy gap to CPNN places the biradical's excited states significantly below the DBH S_1 origin energy. Moreover, the DBH S_1 state adiabatically correlates with the singlet excited biradical, marked S_2 CPNN in Figure 5.⁴⁰ Quantum chemical considerations therefore disclose a photochemically accessible state of the CPNN biradical whose C–N–N structure is linear. We propose that gas-phase S_1 DBH molecules decay to that S_2 state of the CPNN diazenyl biradical. This intermediate then rapidly intersystem-crosses to the nearby T_1 CPNN state, whose C–N–N angle should also be linear or near-linear. From this state, electronic predissociation into ground-state N_2 and T_0 CPD occurs with minimal rotational excitation of the N_2 .

Several aspects of this proposed mechanism deserve comment. Although the S_2 state of the CPNN biradical lies lower in energy on the same adiabatic potential surface as the DBH S_1 state, we expect that a small activation barrier must be surmounted to reach S_2 CPNN from S_1 DBH. If there were no such barrier, the absorption spectrum of DBH would appear diffuse rather than structured and the fluorescence lifetime would be much shorter than the observed 2 ns. Even though we irradiate DBH at its 0–0 band, a large fraction of the S_1 molecules may contain vibrational energy that was present as thermal population of low-frequency ground-state modes and was transferred to S_1 through excitation of overlapping sequence bands. This vibrational excitation may account for the collision-free bond cleavage of our photoexcited DBH. Figure 5 suggests that after the S_2 CPNN intermediate undergoes intersystem crossing to T_1 CPNN, relaxation might continue to the lower lying and correlated T_1 state of DBH. However, this step entails reclosure of the broken C–N bond and is entropically inhibited because it requires a return to the very specific strained structure of DBH starting from the large set of relaxed conformations represented by the sketch of Figure 6.

Another concern is understanding why the CPNN biradicals do not undergo internal conversion from T_1 to T_0 , a process asserted by Reedich and Sheridan to be very rapid because the corresponding surfaces become degenerate in linear geometries of model radical systems such as HCO and HNN.^{35,43} One expects that dissociation of the radical on its bent ground-state surface will occur promptly after such internal conversion. We note that this very process has recently been studied by Houston and co-workers for the HCO radical optically excited to its low-lying linear excited state (the analogue of T_1 in DBH).⁴⁴ As expected for dissociation that follows internal conversion from a linear to a bent state, the nascent rotational distribution measured

for the CO was highly excited: far hotter than the distribution we find for N_2 from DBH and even more energetic than that of N_2 from the methyldiazenyl radical. These findings support the view that photofragment rotational distributions reflect the structure of the dissociating species and that DBH does not dissociate through the bent diazenyl ground state. It seems likely that, in contrast to the suggestion of Reedich and Sheridan, HCO is too different from the CPNN biradical to serve as a model for the diazenyl's radiationless relaxation. Weak interactions between the two radical centers of CPNN plus its lack of cylindrical symmetry may split the degeneracy present in HCO and significantly slow the rate of CPNN internal conversion.

When Solomon et al. first reported the quenching of S_1 emission by added buffer gases, they explained the effect as collision-induced dissociation.⁵ We think this explanation is plausible, because collisions could assist the formation of the C_1 -symmetry biradical either by providing activation energy or by breaking the C_2 symmetry of DBH. However, experimental evidence^{6–10} shows that the solution-phase mechanism differs from the low-pressure mechanism in bypassing the formation of T_0 CPD. In addition to quenching fluorescence, collisions may also induce rapid production of the S_1 CPNN diazenyl biradical, leading to products similar to those found in thermolysis.

One intriguing measurement is the lifetime of the nitrogen precursor in DBH, which at 25 ns is 5 times greater than the lifetime of the methyldiazenyl radical formed in azomethane photolysis. If these two diazenyl radicals shared a common dissociation mechanism, then the one from DBH should be shorter lived than methyldiazenyl because the incipient CPD (a secondary radical) is more stable than methyl. The observed violation of this expected pattern suggests that different mechanisms operate. We propose that the dissociative transition from T_1 CPNN to T_0 CPD should be viewed as a surface-crossing predissociation between states that are not adiabatically correlated, in contrast to the adiabatic dissociation of methyldiazenyl. We interpret the nascent rotational and vibrational distributions of N_2 as reflecting the critical configuration at which this predissociation most frequently occurs. In this way the critical structure is analogous to the transition state of an adiabatic process, and for DBH dissociation, the critical configuration would be intermediate in structure between T_1 CPNN and T_0 CPD plus free N_2 . From the measured rotational and vibrational nascent distributions we infer a critical configuration having a linear C–N–N angle and an N–N separation of $1.13 \pm 0.01\text{ \AA}$. This distortion from the T_1 CPNN structure is probably small enough to be energetically accessible even though continued stretching of the C–N bond of T_1 CPNN leads adiabatically to an electronically excited state of N_2 .^{41,45} A key factor in making predissociation from T_1 CPNN to T_0 CPD seem plausible is the estimated 51 kcal/mol exothermicity of this step.

Our suggested photochemical mechanism for S_1 DBH is similar to that proposed by Adam and co-workers.⁹ Like our mechanism, theirs includes two steps of C–N bond breaking to form first a diazenyl biradical intermediate and then the T_0 CPD biradical. However, the two schemes differ in that Adam and co-workers showed the second step occurring from the lowest triplet state of the diazenyl biradical, in parallel with a minor channel involving the diazenyl singlet state. The mechanism shown in Figure 6 is consistent with the gas-phase experiments of Roth and Martin.⁴⁶ These workers found equal quantities of exo and endo BCP after photolyzing deuterium-labeled DBH samples, a result that would be expected if BCP is formed from a planar precursor such as T_0 CPD. Our proposed scheme also agrees with the conclusion of Steel and co-workers, based largely on oxygen quenching results, that the T_1 state of DBH does not participate in direct photolysis.^{5,33}

Why does the photochemistry of DBH differ from that of acyclic azoalkanes? A major influence is probably the large release

(43) Tanaka, K.; Davidson, E. R. *J. Chem. Phys.* **1979**, *70*, 2904.

(44) Kable, S. H.; Loison, J.-C.; Houston, P. L. *J. Chem. Phys.* **1990**, *92*, 6332.

(45) Vasudevan, K.; Peyerimhoff, S. D.; Buenker, R. J. *J. Mol. Struct.* **1975**, *29*, 285.

(46) Roth, W. R.; Martin, M. *Justus Liebigs Ann. Chem.* **1967**, *702*, 1.

of ring strain energy that occurs as the first C-N bond of DBH is broken. As seen in Figure 5, this exothermicity lowers the energies of diazenyl states relative to DBH and makes the lowest excited diazenyl states energetically accessible. By contrast, acyclic azoalkanes prepared in their S_1 states cannot form electronically excited diazenyl radicals.¹⁸ It seems likely that vapor-phase DBH shows an anomalously long S_1 lifetime and a structured absorption spectrum because its rigid covalent bridges prevent excited-state motion along the cis-trans twisting coordinate. In addition, this structural constraint would prevent DBH from photodissociating through twisted conformations, as we suspect occurs in acyclic azoalkanes.

The photodissociative quantum yield of DBH is much higher than that of the related compound 2,3-diazabicyclo[2.2.2]oct-2-ene (DBO), even though the two molecules differ by only one methylene group.³³ This surprising difference in behavior may be rationalized by using the same energetic and correlation considerations discussed above. Compared to DBH, the lower S_1-S_0 energy gap and higher thermolysis activation barrier of DBO combine to place its linear excited diazenyl biradical state approximately 5 kcal/mol higher than its S_1 origin energy. Thus, like DBH, optically excited DBO is inhibited from twisting about its double bond; but unlike DBH, it cannot reach the electronically excited diazenyl biradical and therefore has no adiabatic route for bond cleavage. With both of these decay channels obstructed, S_1 DBO shows an anomalously long lifetime and the highest fluorescence quantum yield known for any azoalkane.³³

Conclusions

The photochemistry of DBH vapor excited to the origin of its S_1 state has been investigated by time-resolved spectroscopy on the nanosecond scale. Fluorescence lifetime measurements show the optically prepared state to undergo collision-free decay with a characteristic lifetime of slightly more than 2 ns. Time-resolved CARS measurements reveal that molecular nitrogen is produced from a precursor whose lifetime is approximately 25 ns. The

unrelaxed nitrogen photoproduct molecules, when compared to those formed from azomethane, show a very similar vibrational state distribution but a significantly cooler rotational distribution. CARS spectroscopy has been used to monitor appearance kinetics of the bicyclopentane photoproduct, revealing a precursor lifetime of 195 ns. We interpret this value as the first-order lifetime of the triplet 1,3-cyclopentanedyl biradical against decay through ring closure.

The photochemical mechanism proposed to account for these findings involves stepwise breaking of the two C-N bonds. We view the first step as adiabatic formation of an excited singlet state of the diazenyl biradical from optically prepared S_1 DBH. The excited diazenyl singlet is then thought to undergo rapid intersystem crossing to the corresponding excited diazenyl triplet, which lives for 25 ns before predissociating into N_2 plus the lowest triplet state of the 1,3-cyclopentanedyl biradical. We interpret the cool rotational distribution of the N_2 photoproduct as reflecting the linear C-N-N structure that is characteristic of the predissociating diazenyl excited state.

These findings and the proposed mechanism apply to vapor-phase photodissociation of S_1 DBH in the presence of low to moderate buffer gas pressures, but not necessarily to solution photolysis, where a singlet channel seems to dominate. Further time-resolved experiments capable of intercepting diazenyl intermediates will be needed to understand this difference and to confirm the proposed gas-phase mechanism.

Acknowledgment. We are grateful to the National Science Foundation and the Robert A. Welch Foundation for research support. Our time-resolved fluorescence data were obtained at the Center for Fast Kinetics Research, which is supported jointly by the Biomedical Research Technology Program of the Division of Research Resources of NIH (RR00886) and by the University of Texas at Austin. We are also pleased to thank B. K. Andrews and K. A. Burton for valuable discussions and for their computational and experimental contributions.

Structures of X_2F_4 , from Carbon to Lead. Unsaturation through Fluorine Bridges in Group 14

Georges Trinquier* and Jean-Claude Barthelat

Contribution from the Laboratoire de Physique Quantique, C.N.R.S., U.R.A. No. 505, Université Paul-Sabatier, 31062 Toulouse Cedex, France. Received January 5, 1990

Abstract: The various isomers of X_2F_4 with $X = C, Si, Ge, Sn,$ and Pb are investigated through ab initio calculations using effective core potentials and taking into account part of the relativistic effects for tin and lead atoms. Geometries are determined at the SCF level and their relative energies are refined through CI calculations. The planar π -bonded structure $F_2X=XF_2$ is found to be a true minimum on the C_2F_4 potential energy surface, a saddle point on the $Si_2F_4, Ge_2F_4,$ and Sn_2F_4 surfaces, and a true minimum on the first singlet excited Pb_2F_4 surface. The F_3X-XF isomer is found to be a true minimum in all cases but lead. Two nearly degenerate doubly bridged structures, cis and trans, are found to be true minima in all cases but carbon. The preferred isomers are tetrafluoroethylene for C_2F_4 , tetrafluorosilylsilylene for Si_2F_4 , and the trans-bridged structures for $Ge_2F_4, Sn_2F_4,$ and Pb_2F_4 . The diradical triplet species F_2X-XF_2 are always found to be significantly higher in energy than the preferred singlet ground-state forms. With respect to two singlet XF_2 fragments, the bridged structures have binding energies that increase regularly along the series from 3 kcal/mol in Si_2F_4 to 62 kcal/mol in Pb_2F_4 , whereas bridged C_2F_4 is largely unbound. The potential wells corresponding to the bridged structures are found to be rather flat, possibly inducing small distortions associated to very slight energy changes. The in-plane $C_{2h} \rightarrow C_i$ deformation found for the planar four-membered ring of Ge_2F_4 is in agreement with its solid-state geometry. A structural and energetic comparison is made within group 14 between the fluorine bridges in X_2F_4 and the hydrogen bridges in X_2H_4 . Some results are compared with spectroscopic data available for the monomers and dimers of SnF_2 and PbF_2 .

1. Introduction

While tetrafluoroethylene has been the target of many theoretical studies related to its structure^{1,2} or its weak C=C bond

energy,³⁻⁵ there is much less structural and theoretical work on its heavier analogues in group 14. For Si_2F_4 , a doubly bonded

(1) Dixon, D. A.; Fukunaga, T.; Smart, B. E. *J. Am. Chem. Soc.* **1986**, *108*, 1585.

(2) Heaton, M. M.; El-Talbi, M. R. *J. Chem. Phys.* **1986**, *85*, 7198.

(3) Carter, E. A.; Goddard, W. A., III. *J. Am. Chem. Soc.* **1988**, *110*, 4077.

(4) Schultz, P. A.; Messmer, R. P. *J. Am. Chem. Soc.* **1988**, *110*, 8258.

(5) Wang, S. Y.; Borden, W. T. *J. Am. Chem. Soc.* **1989**, *111*, 7282.